Annu. Rev. Biophys. Biomol. Struct. 1997. 26:157–79

STRUCTURAL PERSPECTIVES OF PHOSPHOLAMBAN, A HELICAL TRANSMEMBRANE PENTAMER

Isaiah T. Arkin
Howard Hughes Medical Institute and Department of Molecular Biophysics and Biochemistry, Yale University, New Haven, Connecticut 06520

Paul D. Adams
Department of Molecular Biophysics and Biochemistry, Yale University, New Haven, Connecticut 06520

Axel T. Brünger
Howard Hughes Medical Institute and Department of Molecular Biophysics and Biochemistry, Yale University, New Haven, Connecticut 06520

Steven O. Smith
Department of Molecular Biophysics and Biochemistry, Yale University, New Haven, Connecticut 06520

Donald M. Engelman
Department of Molecular Biophysics and Biochemistry, Yale University, New Haven, Connecticut 06520

KEY WORDS: membrane protein, ion channel, calcium regulation, sarcoplasmic reticulum, transmembrane helices

ABSTRACT

Phospholamban is a 52-amino-acid protein that assembles into a pentamer in sarcoplasmic reticulum membranes. The protein has a role in the regulation of the resident calcium ATPase through an inhibitory association that can be reversed by phosphorylation. The phosphorylation of phospholamban is initiated by β-adrenergic stimulation, identifying phospholamban as an important component in the stimulation of cardiac activity by β-agonists. It is this role of phospholamban that has motivated studies in recent decades. There is evidence that phospholamban may also function as a Ca^{2+}-selective ion channel. The structural

1056-8700/97/0610-0157$08.00

properties of phospholamban have been studied by mutagenesis, modeling, and spectroscopy, resulting in a new view of the organization of this key molecule in membranes.

CONTENTS

INTRODUCTION

Phospholamban was discovered in 1974 as one of the major proteins phosphorylated upon adrenergic stimulation of the cardiac myocyte (36, 41). It was, therefore, appropriately named the phosphate receiver ($\lambda\alpha\mu\beta\delta\nu\omega$ = to receive). Since adrenergic stimulation is a unique feature of cardiac muscle physiology, phospholamban received considerable attention from the research community concerned with cardiac function.

Phospholamban is found in the sarcoplasmic reticulum of cardiac (36, 41) and smooth muscle (54). Its presumed function is the regulation of the resident Ca^{2+}-pump by way of an inhibitory association of the two proteins that is abolished upon phospholamban phosphorylation (30) by c-AMP and Ca^{2+}/calmodulin-dependent protein kinases in additive fashion (61). Phospholamban has also been associated with ion channel activities in lipid bilayer membranes (42). The structure of phospholamban that emerges from current studies seems compatible with a possible transmembrane channel function, raising a number of issues concerning ion channel structure and function.

Phospholamban is a small (52 amino acids) transmembrane protein that assembles into stable pentamers. Its small size makes it amenable to relatively simple applications of spectroscopic methods and computational modeling. The combination of spectroscopy and modeling has led to a view of phospholamban structure that is helpful in refining ideas concerning membrane protein structure and oligomerization as well as providing a basis for thinking about its functions.

We discuss the model that has emerged from a combination of spectroscopy (4), molecular modeling (1), and mutagenesis (2). The resulting model allows

a discussion of the electrostatics of the protein (3), which emphasizes the importance of oligomeric structure in ion channels and also the potential roles of configurational and mutagenic changes at remote locations on the electrostatic potentials found in ion channels.

PHOSPHOLAMBAN STRUCTURE

The small size of phospholamban and its functional importance attract considerable research. Structural studies of phospholamban, however, have been hindered by the difficulty in purifying a very small, highly hydrophobic protein. Purification of phospholamban is by no means a trivial effort (5, 10, 33, 45). Methods for purification have included the use of organic solvents (7, 23), sulfhydryl affinity chromatography (34), and monoclonal antibody columns (55, 60).

Heterologous expression efforts, initially in *Escherichia coli*, were not successful (12). Expression in baculovirus has been more fruitful (55), and functional expression also has been possible in low amounts in COS-1 cells (15). More recently, the chemical synthesis of the entire protein has been reported (72), providing large amounts of highly purified protein, and site-specific isotopic labels (4, 48).

Sequence analysis of phospholamban has shown that the protein contains two distinct segments. The cytoplasmic segment corresponds to roughly the amino terminal half of the protein, thereby categorizing phospholamban as a type II membrane protein. This segment contains S16 and T17, residues phosphorylated by cAMP and Ca^{2+}/calmodulin-dependent protein kinases, respectively (57). The carboxy terminal half of the protein is extremely hydrophobic and traverses the bilayer as a transmembrane α-helix (4). It contains three cysteine residues C36, C41, and C46 that are all thought to be in reduced form. Acetylation of the amino terminal methionine also occurs (13).

Phospholamban Primary Structure

cDNA sequences are available for several mammalian and avian species: canine (16, 67, 68), pig (71), rabbit (14, 44), human (17), rat (27), mouse (18), and chicken (66). Complete genomic sequences are available for rabbit (17), chicken (66), and rat (13, 32, 57). No signal sequence is found in the gene, and no introns are found in the coding region.

Phospholamban sequences are highly conserved (Figure 1). The sequence of chicken phospholamban is highly similar (85%) to its mammalian counterparts. The human phospholamban gene is mapped to chromosome band 6q22.1, while that of the Ca^{2+}-pump and calsequestrin map to 12q23-q34.1 and 1q21, respectively (50).

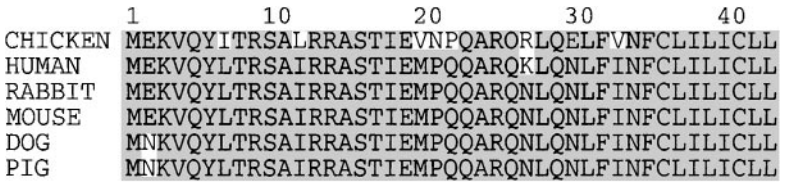

Figure 1 Sequence alignment of phospholamban. Phospholamban sequences are aligned according to sequence homology. Shaded regions indicate identity. Note that the sequence of pig phospholamban is identical to that of dog, while the sequence of rabbit phospholamban is identical to that of rat and mouse. See text for references.

Phospholamban Size Determination

One of the most intriguing elements in phospholamban structure is its oligomeric nature (see Table 1).

The oligomeric state of phospholamban (as detected by SDS-PAGE) changes as a function of sample handling. Boiling reduces the apparent size of the protein reversibly (43), while addition of Mg^{2+} ions reverses the monomerizing process (47). Reducing agents do not affect oligomerization, suggesting that it is not caused by disulfide bond formation (Table 1). The most populated forms of phospholamban on SDS-PAGE are those of monomer and pentamer (72).

Further evidence that the protein is a pentamer came from phosphorylation experiments followed by observing mobility retardation of the pentamer band. In these studies both cAMP and Ca^{2+}/calmodulin-dependent protein kinases were used [phosphorylation of S16 and T17, respectively (57)], resulting in the appearance of eleven different bands (19, 28, 75). These bands were assumed to represent a pentameric complex with different phosphorylation levels ranging from zero to ten phosphates per complex. This stoichiometry is what one would expect for a pentamer where each monomer contains two phosphorylation sites, as shown in Figure 2.

Table 1 Representative molecular weights of phospholamban determined from SDS-PAGE

Molecular weight (SDS-PAGE)	Reference
24,000 and 9000	43
22,000 and 6000	6
26,000 and 6000	13
27,000 and 11,000	29
24,500 and lower than 14,400	28
23,000; 11,000; 8000; and 4000	47
22,000; 11,000; and 5500	40

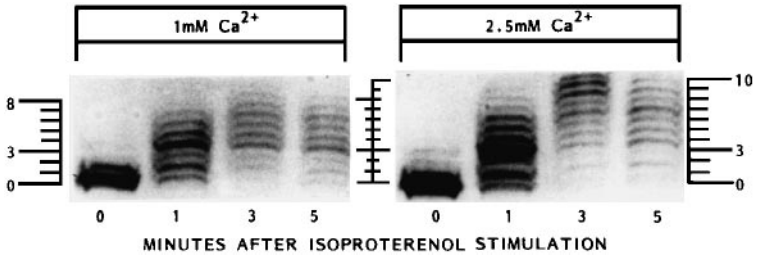

Figure 2 Western blotting SDS-PAGE of phospholamban. Isolated SR vesicles were subjected to phosphorylation induced by isoproterenol, and after the times indicated were electrophoresed and developed with anti-phospholamban antibodies. The 11 discrete mobilities correspond to the 11 different phosphorylation levels of a pentameric protein containing 2 phosphorylation sites per protomer. Figure reproduced with permission (75).

Trypsin cleavage generates a peptide that encompasses the transmembrane domain of phospholamban (residues 25–52) (42). This peptide oligomerizes in SDS-PAGE, and although it is only half the size of full-length phospholamban, the increase in apparent mobility is minimal (42). This is another example of anomalous migrations of membrane proteins in SDS-PAGE. No oligomerization is seen in a peptide corresponding to the cytoplasmic domain (residues 1–31) (39), providing evidence that the pentamerization of phospholamban is solely a function of its transmembrane segment.

Takagi and colleagues (73), using low-angle laser light scattering and high-performance gel permeation chromatography, were able to determine the molecular weight of phospholamban in SDS micelles as 30.4 kDa, expected from a pentamer of phospholamban monomers.

Attempts have also been made to determine the oligomeric state of phospholamban in environments other than sodium dodecyl sulfate micelles. Pentamerization was observed in n-octyl-β-glucoside micelles by gel permeation chromatography (21). Analytical centrifugation in methanol and in $C_{12}E_8$ detergent micelles provided evidence that under those conditions the molecular weights of the protein are 12.3 kDa and a combination of 6 kDa and 30 kDa, respectively (72). Radiation inactivation studies were able to show energy transfer only between a dimer of proteins, while in the case of the glucose transporter, energy transfer occurred between the 12 putative transmembrane helices (31).

Secondary Structure

Circular dichroism spectra of phospholamban in detergent micelles as well as of the tryptic peptide corresponding to residues 25–52 have been reported (59). The

spectra were similar in each of the detergents used ($C_{12}E_8$, sodium dodecyl sulfate, and n-octyl-β-glucoside) and exhibited features similar to those of other highly helical proteins. Helicity increased in the tryptic fragment of phospholamban corresponding to the transmembrane domain relative to full-length protein (59). No decrease in secondary structure is present upon boiling the sample.

Studies investigating the merits of determining the secondary structure estimation of membrane proteins based on circular dichroism results have shown that this is exceptionally difficult to quantitate (51). Carafoli and colleagues, studying the secondary structure of synthetic phospholamban in $C_{12}E_8$ detergent micelles, obtained similar results (72). The results of this analysis of secondary structure content have led Jones and colleagues to derive a model for this pentamerizing protein (59, 74). In this model the protein is seen as a bundle of five transmembrane α-helices connected to a small cytoplasmic α-helix by a stretch of random or β-sheet amino acids.

Circular dichroism spectra have been obtained for Plb WT (phospholamban wild type) reconstituted in phospholipid bilayers (Figure 3) (4). Although no quantitation of secondary structure was made, qualitatively it can be seen that the protein contains a significant percentage of helical structure. Furthermore a thermal scan recording ellipticity at 222 nm revealed no loss of helicity when recorded in the temperature range scanned (37–95°C).

Such resistance to thermal denaturation is not uncommon in membrane proteins, as the helices are stabilized by strong hydrogen bonding in a nonpolar environment. Circular dichroism studies of the cytoplasmic peptide (residues 1–25) (24) or of a larger fragment (residues 2–33) (64) as well as NMR studies

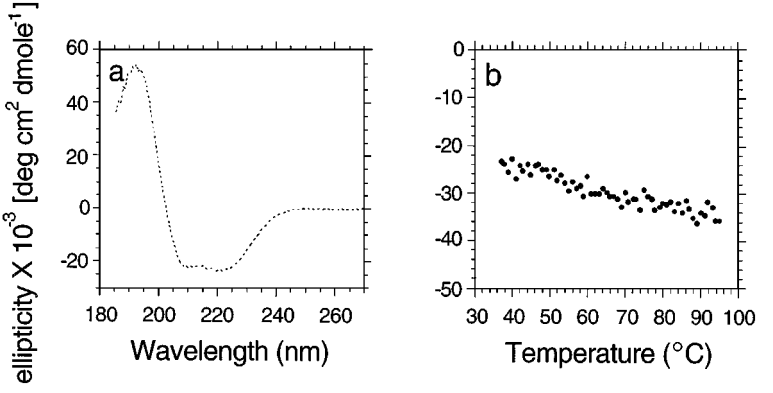

Figure 3 (*a*) Circular dichroism spectrum of PlbWT in DMPC vesicles scaled to mean residue ellipticity. The spectrum was obtained at 37°C in 0.2 mM Tris·HCL, pH 7.4. (*b*) Ellipticity thermal profile of PlbWT at 222 nm.

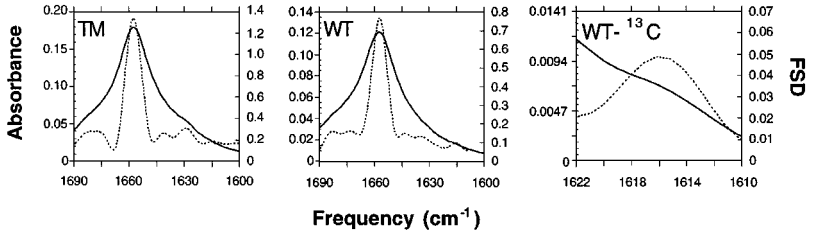

Figure 4 Transmission FTIR spectra and Fourier self-deconvolutions of PlbTM and PlbWT. The transmission FTIR spectra of PlbTM (*left*) and PlbWT (*middle*) are drawn in solid lines, while Fourier self-deconvolutions are drawn in dotted lines. An expansion of the region of the spectrum of PlbWT that includes the ^{13}C isotope-shifted band (*right*).

in solution (24) (residues 1–25), have shown that the peptide adopts a denatured conformation in aqueous solution. Addition of trifluoroethanol to this solution (24, 64), a nonspecific helix-promoting solvent (e.g. 11, 53, 65, 76), induces α-helix formation.

Fourier transform infrared (FTIR) spectroscopy (4, 63) has been used to determine secondary structure on the basis of the shape and frequency of the amide I vibrational mode (Figure 4). Orientation of the secondary structure elements is determined from the difference in absorption of parallel and perpendicular polarized light (dichroic ratio, R^{ATR}) of an oriented protein sample (Figure 5). Since membranes and lipid bilayers tend to form ordered stacks when deposited on surfaces, FTIR can be exceptionally useful. (For a review on the analysis of membrane protein structure by FTIR, see 8.) In two studies on the secondary structure of phospholamban, FTIR spectra of the full-length protein have been compared to spectra of a peptide encompassing the transmembrane domain of the protein (residues 25–52).

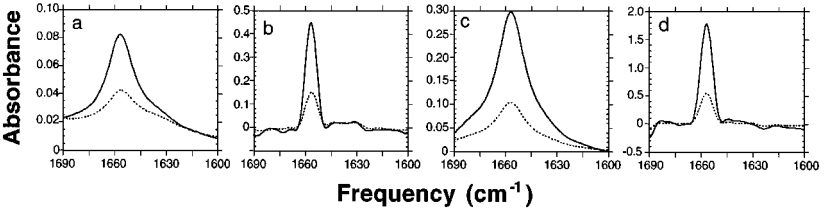

Figure 5 Polarized ATR-FTIR spectra and Fourier self-deconvolutions of PlbTM and PlbWT. The polarized ATR-FTIR spectra of PlbTM (*a*) and PlbWT (*c*) were obtained using parallel (solid line) or perpendicular (dotted line) polarized light. The Fourier self-deconvolutions (37) of PlbTM (*b*) and PlbWT (*d*) were obtained with a bandwidth of 13 cm^{-1} and an enhancement factor of 2.4 (9).

Table 2 Secondary structure analysis by FTIR of phospholamban in phospholipid bilayers from Arkin et al (4) and Tatulian et al (63)

Parameter	Arkin et al (4)	Tatulian et al (63)
Helical amide I intensity, PlbTM	67%	73%
Helical amide I intensity, PlbWT	65%	64%
Calculated helicity, PlbTM	79% (22/28)	73% (20/28)
Calculated helicity, PlbWT	77% (40/52)	64% (33/52)

Secondary structure The results of the two studies pertaining to secondary structure assignments are listed comparatively in Table 2. The estimates of helical content based on the amide I vibrational mode is similar in both studies within experimental error. The derived helical percentages are different because Arkin et al (4) took into account the differences between the extinction coefficients of the different structure elements (4), as well as contributions from overlapping side chain modes, which can be as much as 25% (35, 69, 70). Thus, it is not surprising that the helical percentages would be lower in Tatulian et al's (63) study than in Arkin's.

Helix orientation The results of the two studies pertaining to helical orientation are listed comparatively in Table 3. As the two groups have used different sample geometries (single bilayers as opposed to multilayers), comparisons between the measured dichroic ratios are not straightforward. This is a result of the different assumptions made in the calculation of the electric field amplitudes of the evanescent wave [thick film versus thin film approximation (22)].

Comparisons of the derived order parameters have led to different structural models for the protein. Tatulian et al (63) have proposed that phospholamban is composed of two disjointed helices: a perpendicular transmembrane helix and a tilted cytosolic helix connected by a two stranded β-sheet, as shown

Table 3 Helical orientation analysis by ATR-FTIR of phospholamban in phospholipid bilayers from Arkin et al (4) and Tatulian et al (63)

Parameter	Arkin et al (4)	Tatulian et al (63)
R_{max}^{ATR} of PlbWT	3.31	2.39
Order parameter of PlbWT ($\alpha = 39^\circ$)	0.68	0.52
R_{max}^{ATR} of PlbTM	3.43	3.26
Order parameter of PlbTM ($\alpha = 39^\circ$)	0.72	0.95
R_{max}^{ATR} of the Lipids	0.94	1.27
Order parameter of the Lipids ($\alpha = 90^\circ$)	0.89	0.47
Lipid ν_{CH_2} symmetric stretch	2852 cm^{-1}	2851 cm^{-1}

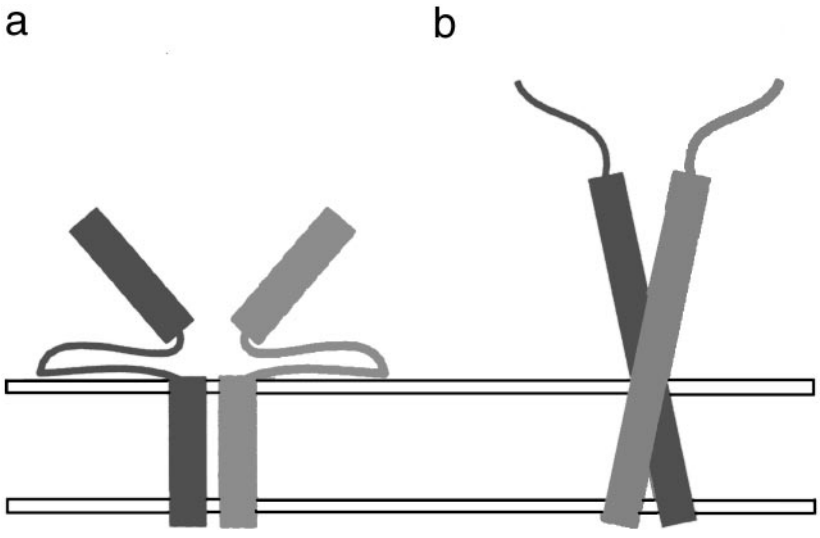

Figure 6 Model of the phospholamban ion channel complex. (*a*) Model by Tatulian et al (63). (*b*) Model by Arkin et al (4). For ease of presentation, only two protomers out of five are shown in two different shades of grey.

in Figure 6*a*. A possible weakness of this model is that the cytosolic helix, presumed by Tatulian et al (63) to be a stable independent domain, is found to be in random-coil configuration when synthesized on its own.

Arkin et al (4) propose a continuous α-helix, half of which is transmembrane, and the other half cytosolic, as shown in Figure 6*b*. This model is consistent with the high heat lability of the complex (see Figure 3*b*). A possible weakness in this model is that proline 21 must be accomodated in a helix, probably distorting the structure.

In a more recent study by Rothschild and coworkers (48), detailed FTIR studies were undertaken on the transmembrane domain of phospholamban (residues 25–52). The orientation of the transmembrane domain was measured by attenuated total internal reflection (ATR) and tilted transmission polarized spectroscopy (56). The results gave higher tilt angles from the lipid bilayer normal ($48 \pm 1^{\circ}$).

Rothschild and coworkers also utilized site-specific isotope labeling in conjunction with FTIR. ^{13}C carbonyls introduced at positions L39 and L42 result in a shift of the amide I vibrational mode to 1614 cm^{-1}, indicating that those two sites are in helical secondary structure (62). Furthermore, the region between L39–C46 may be helical, since the N-H groups on L43 and C46 to

which the ^{13}C carbonyls are hydrogen bonded must also be part of the helical structure.

Phosphorylation Effect on Phospholamban Structure

Phosphorylation is the regulatory switch of phospholamban. It confers protease resistance, suggesting a change in the structure of the protein (25). However, circular dichroism measurements show no difference upon phosphorylation (59). One might envision a model whereby phosphorylation would cause only a change in the tertiary structure of the protein (e.g. tilting of the helices) that would not be detected by circular dichroism. Alternatively, changing the pI of the protein by more than five units, as well as inserting two bulky phosphate groups per protomer, might simply block the protease accessibility without altering the structure of phospholamban.

Studies aimed at elucidating the structure of the cytoplasmic segment of phospholamban either by circular dichroism spectroscopy or by NMR have concluded that this peptide adopts a denatured configuration in aqueous solution (24, 59, 64). Phosphorylation had no effect on these results. The cytoplasmic segment folds into a helical geometry in trifluoroethanol, a helix-promoting solvent, and its structure is observed to change upon phosphorylation. However, the relevance of this change is uncertain because of the solvent environment.

FTIR studies by Tatulian et al (63) and Arkin et al (4) reach different conclusions concerning the effect that phosphorylation has upon the secondary structure and orientation of the secondary structure. Tatulian et al (63) measured a reduction in α-helical content in PlbWT equivalent to six residues. No difference in orientation of the helices was measured in this study. Arkin et al (4) found that phosphorylation did not significantly change the secondary structure of the protein (Figure 7), similar to the result obtained from circular

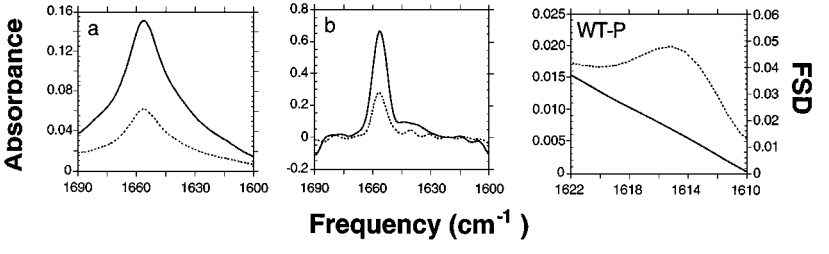

Figure 7 Polarized ATR-FTIR spectra (*a*) and Fourier self-deconvolutions (*b*) of PlbWT-P. Spectra were obtained with parallel (solid lines) or perpendicular polarized light (dotted lines). The far right graph shows an expansion of the parallel polarized ATR-FTIR spectrum in the region of the ^{13}C isotope-shifted amide I mode of PlbWT-P (solid line) and the corresponding Fourier self-deconvolution (dotted line).

dichroism spectroscopy. Furthermore, the use of isotope-edited FTIR (62) lead Arkin et al (4) to conclude that phosphorylation has no effect on the overall secondary structure of the protein or on the local environment near the phosphorylated residues. Similar to results by Tatulian et al (63), no change in helix orientation was observed upon phospholamban phosphorylation.

Environs of the Sulfhydryl Groups

The sulfhydryl groups are the only polar side chains in the phospholamban transmembrane domain. Therefore, Arkin et al (3) have undertaken studies aimed at understanding their structure using FTIR spectroscopy. The vibrational frequencies of all the sulfhydryl stretches have indicated that all of the sulfhydryl protons are strongly H-bonded to carbonyl oxygens located at position $i-4$ in the helix, as predicted previously by molecular modeling (1). This result is consistent with a statistical analysis (20) of cysteine H-bonding, in helices in high resolution structures where more than 72% of all sulfhydryl protons are H-bonded in this way (see Figure 8).

Mutagenesis Effects on Pentamer Formation

Mutagenesis has long been used as a low-resolution tool for analyzing protein structure. The concept behind these studies is to correlate altered properties of a mutated protein with the importance of the site of mutation. The property assayed in the three different mutagenesis studies of phospholamban has been pentamer formation assayed by mobility in SDS-PAGE.

ROLES OF THE AMIDE AND THIOL AMINO ACIDS Phospholamban was expressed, mutagenized, and assessed for pentamer formation in COS-1 cells by

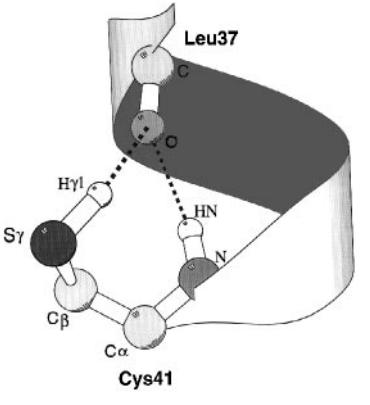

Figure 8 A molecular scheme (obtained with the program Molscript by Per Kraulis) depicting the hydrogen bonding of cysteine 41.

MacLennan and colleagues (15). Attempting to understand the forces behind this non-covalent pentamerization, the researchers mutated two groups of residues. First, they mutated the amide amino acids Q22 and Q23 (Q22A-Q23A and Q22E-Q23E), Q26 and N27 (Q26E-N27D), and Q29 and N30 (Q29E-N30D) in order to determine the importance of the hydrogen-bonding contributions of these residues to pentamer thermal stability (heating the sample prior to electrophoresis). No effect was apparent in any of these mutations.

The second group to be mutated was that of the three cysteine residues in the transmembrane domain of the protein (C36, C41, and C46). Mutations to either alanine or to serine had no effect at ambient temperature at any position, although the thermal stability was affected (in particular, that of C41). Substitutions to phenylalanine had more pronounced effects even at ambient temperatures (e.g. C41F was nearly completely monomeric). Double substitution to alanine was even more deleterious for pentamer formation, reducing the pentamer levels by 50% at ambient temperature, while at elevated temperature it is completely monomeric. A triple substitution of all cysteine residues in phospholamban to alanines resulted in monomeric protein at all temperatures. The authors were therefore able to conclude that although cysteine residues in phospholamban are not responsible for disulfide bond formation, they are important for pentamer stabilization.

AMINO ACIDS RESPONSIBLE FOR PENTAMER FORMATION Engelman and colleagues (3) utilized mutagenesis in an effort to define the interacting surfaces of the pentamerizing transmembrane α-helices of phospholamban. Phospholamban was fused to the carboxy terminus of *Staphylococcal* nuclease, a soluble monomeric protein, and the chimera was expressed in *E. coli*. Phospholamban conferred pentamerizing behavior to the chimeric protein, as seen in Figure 9*a*.

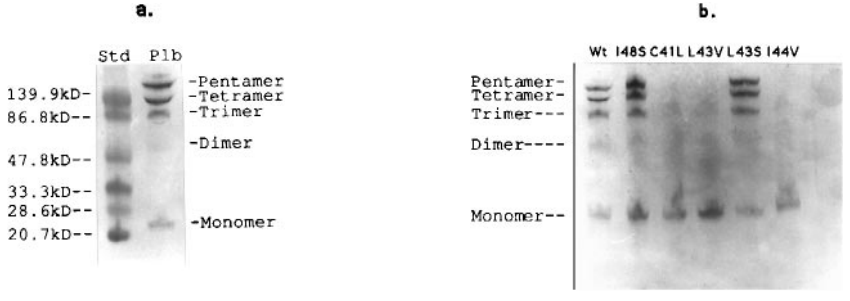

Figure 9 Western blots. A Western blot with anti-nuclease antibodies against whole bacterial lysates derived from glucose-MOPS growths under limiting conditions developed with goat anti-rabbit alkaline conjugate, NBT/BCIP color reaction. (*a*) Wild-type chimeric protein and pre-stained molecular weight markets. (*b*) A selected example of mutant chimeric proteins listing the specific mutation.

Residues in the transmembrane domain were randomly mutated (emphasizing conservative substitutions) and the resulting chimeric proteins were assessed for the ability to pentamerize. A representative gel of the mutant chimeric protein is shown in Figure 9*b*, and tabulation of all of the mutations found is given in Figure 10.

Sensitive, semi-sensitive, and insensitive residues The mutagenesis results point to a pattern of residues, each with different sensitivity toward mutagenesis. Residues such as L37, I40, L44, and 147 were not able to accept any substitutions and retain pentamerizing properties. These sites were therefore labeled sensitive. The degree of specificity at these sites is remarkable. Consider the case of L37, where substitution to its isomer, I, or to M, V, or A each abolished pentamer formation abilities of the resulting chimeric proteins. In contrast, other residues were able to accept any conservative substitution and were labeled insensitive. The third group of residues were those that resulted in different pentameric propensities as a function of the substituted amino acids, and were labelled semi-sensitive.

Sensitivity pattern The resulting pattern of sensitivity (or lack thereof) toward substitution can by analyzed with helical wheel diagrams. Figure 11 presents helical wheel representations at three different pitches: 3.6, 3.5, and 3.9 amino acids per turn. The first corresponds to a canonical helix, while pitches of 3.5 and 3.9 amino acids per turn represent the helix-helix contacts in left-handed coiled-coils and right-handed coiled-coils, respectively.

Phospholamban is a left-handed coiled-coil Helical wheel analysis indicates that residues of equal sensitivity toward substitution (assaying pentamerization)

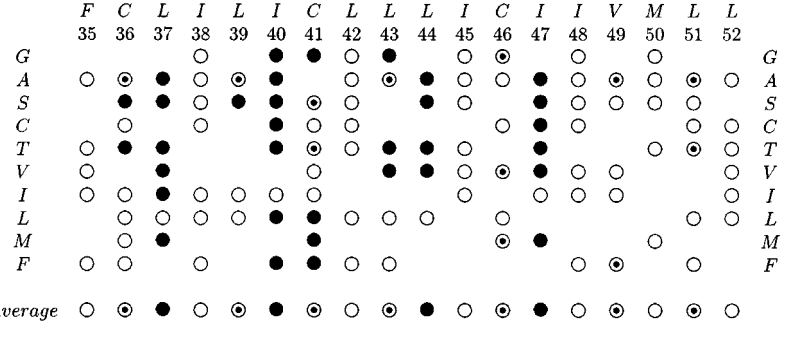

Figure 10 Summary of the effects of conservative substitutions on the oligomeric state of the chimeric protein. Oligomerization properties of point mutants of the phospholamban transmembrane domain were determined by SDS-PAGE/Western blot analysis. Sensitive residues are denoted by filled circles, insensitive residues by open circles, and semi-sensitive residues by semi-filled circles.

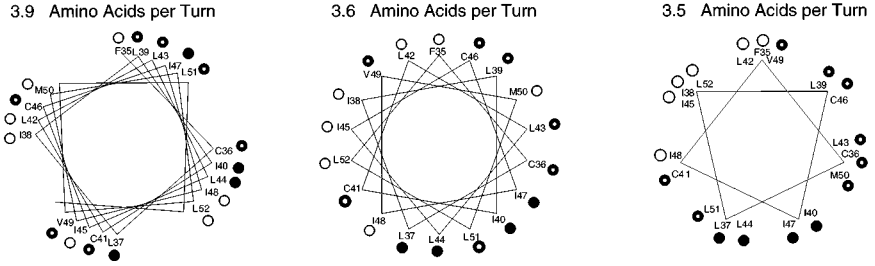

Figure 11 Helical wheel projections. Helical wheel projections at three different pitches: 3.6 (canonical helix), 3.9 (right-handed coiled-coil), and 3.5 (left-handed coiled-coil) amino acids per turn of the transmembrane domain of human phospholamban. Full circles indicate sensitive residues, half-filled circles indicate moderately sensitive residues, and open circles indicate insensitive residues as defined by the mutagenesis. The presumed interaction surface is noted on the 3.5 amino acids per turn projection.

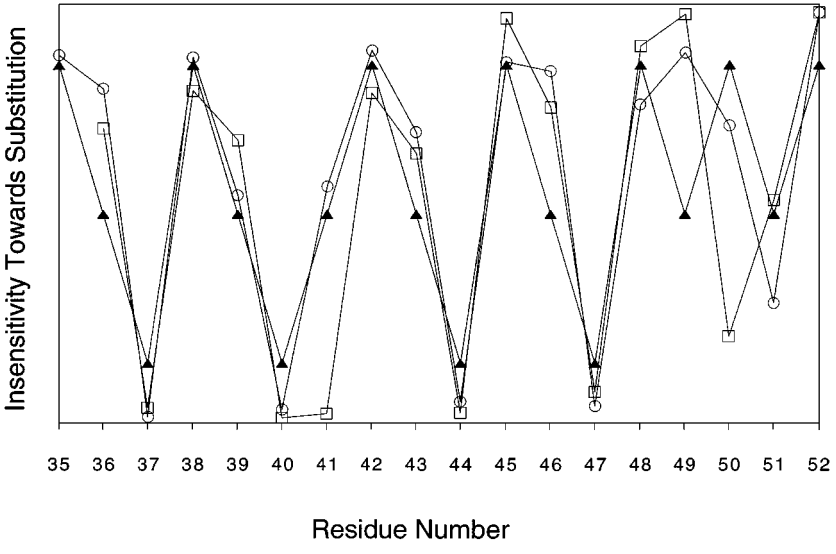

Figure 12 Graph depicting the insensitivity of amino acids in the transmembrane domain of phospholamban toward substitution, when assayed for pentamerization in the two mutagenesis studies. Solid triangles present the results of Engelman and coworkers (3), while open circles represent alanine substitutions, and open squares phenylalanine substitutions (58).

line up on the same faces of the 3.5 amino acids per turn helical wheel diagram, implying that phospholamban is a left-handed coiled-coil.

Jones and co-workers describe additional mutagenesis studies of phospholamban (58). They substituted residues 26–52 of phospholamban with either an alanine or phenylalanine and assayed the in vitro translated proteins by SDS-PAGE. As shown in Figure 12, the results agree remarkably well with the earlier work.

Molecular Modeling

Brünger and colleagues (1) obtained a model for the pentamerizing transmembrane α-helices of phospholamban on theoretical grounds, employing global conformational search methods coupled with molecular dynamics simulations. Starting positions are set at a series of mutual rotations and at both right- and left-handed tilts. Two conceptual approaches were used: One method attempts to identify the most favored structure by extensively exploring the interaction of two monomers; the other examines the interactions in a set of symmetric pentamers. In the case of the dimer search, starting positions were varied at increments of 45° starting from either a left-or right-handed crossing angle (Ω). A number of distinct clusters of structures were obtained (Figure 13*b* and *c*). Average structures were calculated for each of these clusters and were assessed for their ability to form pentamers. The transformation from one helix to the other in the dimer was repeatedly applied to the first helix. The pentamer search was undertaken by concomitantly incrementing the rotational angle between the helices at increments of 20°. Results from this molecular dynamics study are shown in Figure 14.

CORRELATION BETWEEN THE MODELING AND MUTAGENESIS STUDIES As seen in Figures 14*b* and 13*b*, both molecular dynamics search protocols have resulted in several clusters of models. Selection between them on the basis of energy alone (model p4 or d7) yields an interaction energy profile that does not match the sensitivity pattern of the mutagenesis results (see Figure 15*a*). Selection of the model based on the breadth of the energy minimum or, in other words, on the number of models that have clustered at this particular rotational angle, results in a model that fits well with the mutagenesis results (model p1 or d3; see Figure 16*b*).

Two discrepancies between the mutagenesis results and the modeling (as seen in Figure 15*b*) are the higher interaction energy predicted by the modeling for L43 and for the last four residues of the protein in comparison to their sensitivity toward substitution.

Model of the Phospholamban Pentamer

We conclude that the final phospholamban model that best satisfied the data is a left-handed pentamer with a high level of symmetry (Figure 16). The crossing

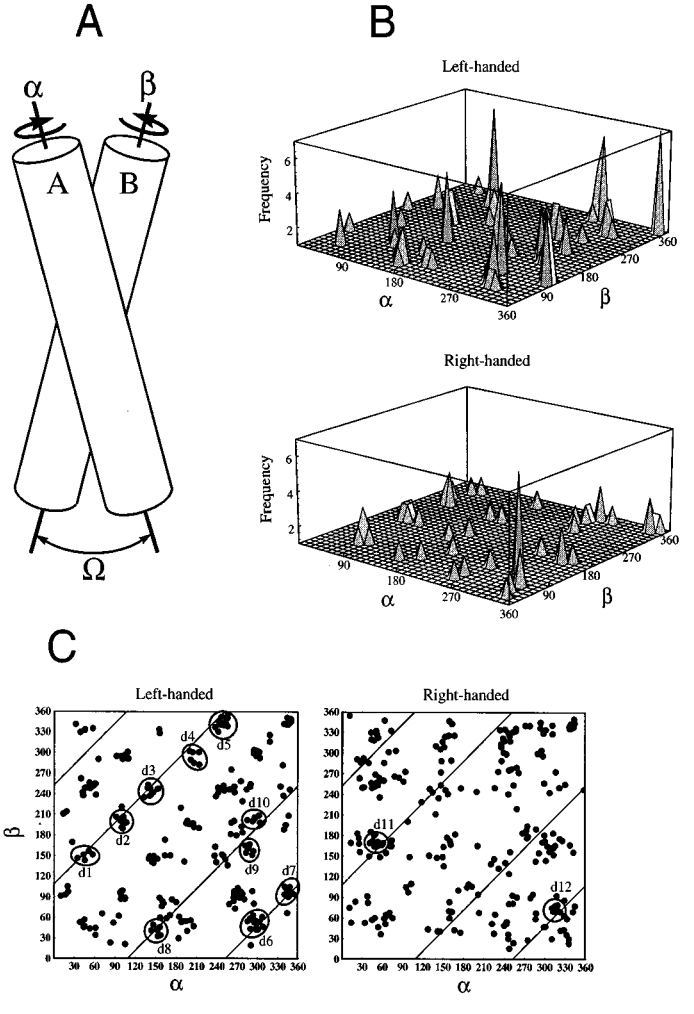

Figure 13 (*a*) The helix rotation parameters α and β were systematically varied in the two-body search. (*b*) Frequency of structures obtained by simulated annealing found in α/β rotation space, averaged over a 10° by 10° grid, for left-handed and right-handed helical pairs. (*c*) Distribution of final α,β rotation angles for all structures obtained by simulated annealing with a final left-handed or right-handed crossing angle. Lines indicate the regions with a pentameric relationship between α and β. The twelve clusters that were consistent with a pentameric interaction are marked (d1–d12). These clusters were used to generate single averaged structures and then refined.

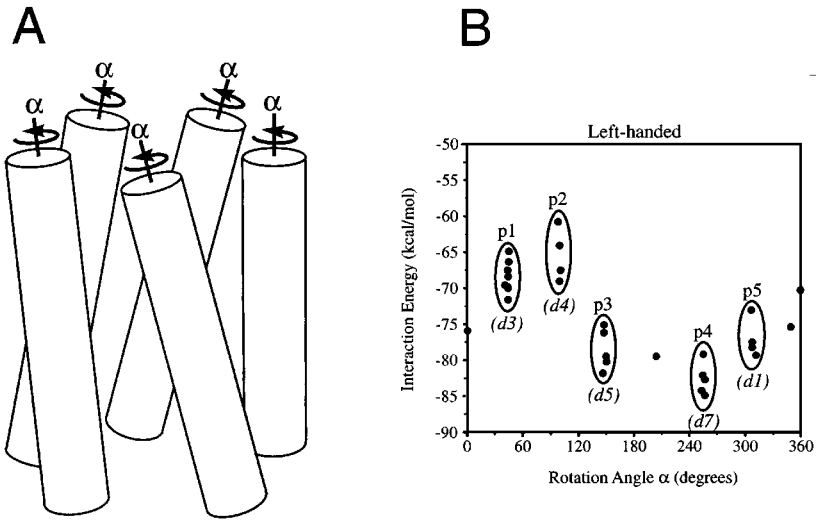

Figure 14 (*a*) The helix rotation parameter α was systematically varied for all helices simultaneously in the symmetric pentamer search. (*b*) Interaction energy vs rotation angle α for left-handed pentamers. The five clusters marked (p1–p5) were used to generate single averaged structures. The lower identifiers (italics) indicate the corresponding dimer models (Figure 13*c*).

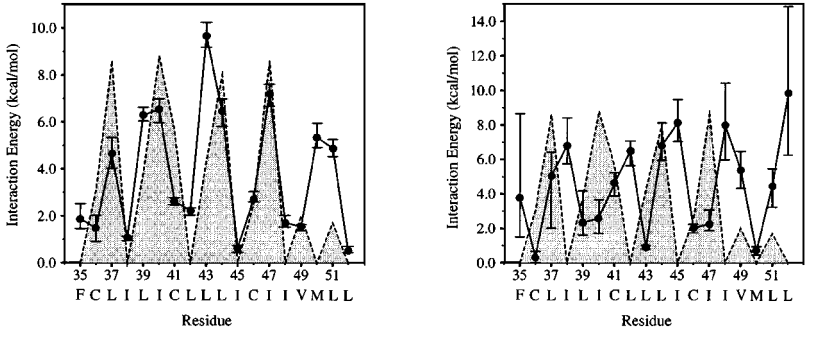

Figure 15 (*a*) Average interaction energy per residue (solid line) compared to the sensitivity of each residue to mutation (dashed line) for the lowest energy model p4. Error bars indicate the minimum and maximum value within the pentamer model. (*b*) As in (*a*) but for model p1.

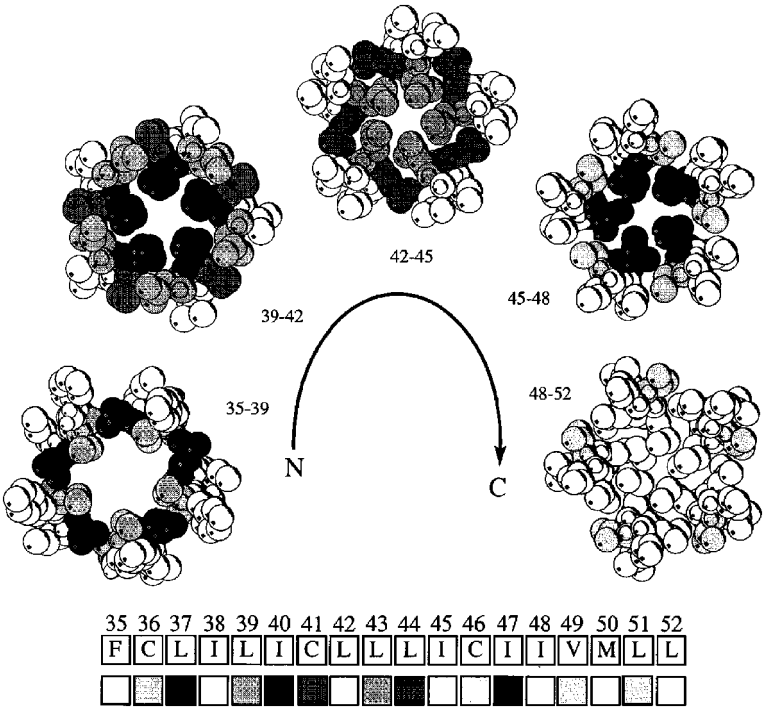

Figure 16 Section through the model p1 (see above), through the pentamer (along the pentamer axis) from the amino to the carboxy terminal. The residues in each section are indicated, their identity and average sensitivity to mutation are shown in the lower scale.

angle between adjacent helices is about 17°, the separation between neighbouring helices is 10 Å, and the average number of residues per turn for each helix is approximately 3.6. These geometric parameters are consistent with a left-handed coiled-coil interaction between the helices and are also similar to results obtained in another, unrelated helix bundle modeling study (38). The models produced from the independent two-body and pentamer searches are very similar to one another, with 0.6 Å rms deviation for Cα atoms and 1.63 Å rms deviation for all atoms (and almost identical geometric parameters). Residues insensitive toward substitution clearly reside on the exterior of the complex, while those found to be sensitive are in the interior. Tight packing interactions between hydrophobic residues hold the complex together. Several residues (as in the case I47) form an interaction ring involving all of the protomers.

A discrete pore is seen through every slice of the model with a diameter ranging between 8 Å and 2 Å, as shown in Figure 17. This pore is too small

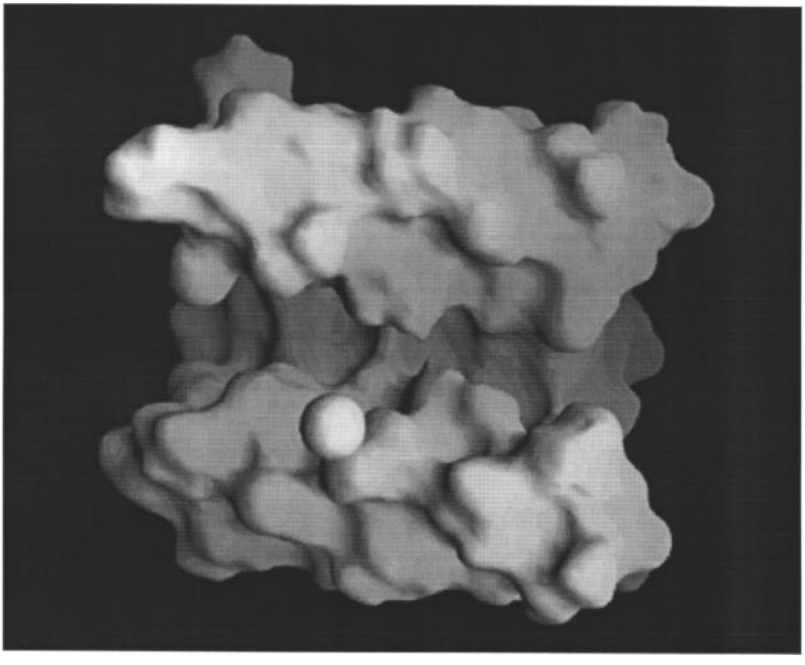

Figure 17 Pore structure. A molecular envelope representation [generated by the program GRASP (49)] for the model derived by molecular dynamics simulations that coincides with the mutagenesis results. One of the monomers was omitted to facilitate viewing of the ion pore. A Ca^{2+} ion is depicted for illustrative purposes. The right side of the figure represents the cytosolic face of the channel, while the left side represents the lumen side.

to accomodate a hydrated calcium ion and might therefore represent the closed state of the channel. This pore is composed almost entirely of hydrophobic groups, and the only polar group is the sulfur of M50 and the thiol group of C36. In any model of the pentamer based on transmembrane helices it is impossible to form a pore lined with polar residues, since the only polar groups in the protein (the thiol groups of the three cysteine residues) do not line up on the same face of a helical wheel.

CONCLUSIONS

Non-covalent interactions between the transmembrane α-helices of phospholamban stabilize a pentameric complex of α-helices. The helical bundle may extend into the cytoplasm, possibly encompassing more than 80% of the protein.

Phosphorylation, the mechanistic "trigger" of the protein, does not seem to cause a conformational change that can be detected by infrared spectroscopy, suggesting that the effect of phosphorylation is mostly electrostatic. Vibrational spectroscopic results show that the sulfhydryl groups located in the transmembrane part of the protein are hydrogen-bonded to the carbonyl oxygen of the $i - 4$ residue. Mutagenesis studies of pentamer disruption result in a sensitivity pattern toward substitution, identifying an interacting protein-protein interaction surface. Molecular modeling approaches coupled with experimental data can yield a model that is interpretable in light of other experimental data, such as the hydrogen-bonding state of transmembrane sulfhydryl protons. Indirect polar effects from amino acids in helices defining a channel can significantly alter the electrostatic field of the channel.

ACKNOWLEDGMENTS

This work was supported by grants from the NIH and NSF, funds from Boehringer Ingelheim Inc. and from the National Foundation for Cancer Research to D.M.E., a grant from the NIH to S.O.S., and by a grant from the NSF to A.T.B. The authors wish to thank Dr. LR Jones for Figure 2 and Dr. EG Kranias for providing unpublished results.

Literature Cited

1. Adams PD, Arkin IT, Engelman DM, Brünger AT. 1995. Computational searching and mutagenesis suggest a structure for the pentameric transmembrane domain of phospholamban. *Nat. Struct. Biol.* 2(2):154–62
2. Arkin IT, Adams PD, MacKenzie KR, Lemmon MA, Brünger AT, Engelman DM. 1994. Structural organization of the pentameric transmembrane alpha-helices of phospholamban, a cardiac ion channel. *EMBO J.* 13(20):4757–64
3. Arkin IT, Adams PD, Aimoto S, Engelman DM, Smith SO. 1996. Structure of the transmembrane cysteine residues in phospholamban. *J. Membr. Biol.* In press
4. Arkin IT, Rothman M, Ludlam CF, Aimoto S, Engelman DM, et al. 1995. Structural model of the phospholamban ion channel complex in phospholipid membranes. *J. Mol. Biol.* 248(4):824–34
5. Bidlack JM, Ambudkar IS, Shamoo AE. 1982. Purification of phospholamban, a 22,000-dalton protein from cardiac sarcoplasmic reticulum that is specifically phosphorylated by cyclic AMP-dependent protein kinase. *J. Biol. Chem.* 257(8):4501–6
6. Bidlack JM, Shamoo AE. 1980. Adenosine 3′,5′-monophosphate-dependent phosphorylation of a 6000 and a 22,000 dalton protein from cardiac sarcoplasmic reticulum. *Biochim. Biophys. Acta* 632(2):310–25
7. Boyot P, Luu B, Jones LR, Trifilieff E. 1989. Purification of phospholamban from bovine cardiac muscle with organic solvents. *Arch. Biochem. Biophys.* 269(2):639–45
8. Braiman MS, Rothschild KJ. 1988. Fourier transform infrared techniques for probing membrane protein structure. *Annu. Rev. Biophys. Biophys. Chem.* 17:541–70
9. Byler DM, Susi H. 1986. Examination of the secondary structure of proteins by deconvolved FTIR spectra. *Biopolymers* 25(3):469–87
10. Capony JP, Rinaldi ML, Guilleux F, Demaille JG. 1983. Isolation of cardiac mem-

brane proteolipids by high pressure liquid chromatography. A comparison of reticular and sarcolemma proteolipids, phospholamban and calciductin. *Biochim. Biophys. Acta* 728(1):83–91
11. Cavatorta P, Sartor G, Neyroz P, Farruggia G, Franzoni L, et al. 1991. Fluorescence and CD studies on the conformation of the gastrin releasing peptide in solution and in the presence of model membranes. *Biopolymers* 31(6):653–61
12. Cook EA, Huggins JP, Sathe G, England PJ, Piggott JR. 1989. The expression of canine cardiac phospholamban in heterologous systems. *Biochem. J.* 264(2):533–38
13. Fujii J, Kadoma M, Tada M, Toda H, Sakiyama F. 1986. Characterization of structural units of phospholamban by amino acid sequencing and electrophoretic analysis. *Biochem. Biophys. Res. Commun.* 138(3):1044–50
14. Fujii J, Lytton J, Tada M, MacLennan DH. 1988. Rabbit cardiac and slow-twitch muscle express the same phospholamban gene. *FEBS Lett.* 227(1):51–55
15. Fujii J, Maruyama K, Tada M, MacLennan DH. 1989. Expression and site-specific mutagenesis of phospholamban. Studies of residues involved in phosphorylation and pentamer formation. *J. Biol. Chem.* 264(22):12950–55
16. Fujii J, Ueno A, Kitano K, Tanaka S, Kadoma M, Tada M. 1987. Complete complementary DNA-derived amino acid sequence of canine cardiac phospholamban. *J. Clin. Invest.* 79(1):301–4
17. Fujii J, Zarain-Herzberg A, Willard HF, Tada M, MacLennan DH. 1991. Structure of the rabbit phospholamban gene, cloning of the human cDNA, and assignment of the gene to human chromosome 6. *J. Biol. Chem.* 266(18):11669–75
18. Ganim JR, Luo W, Ponniah S, Grupp I, Kim HW, et al. 1992. Mouse phospholamban gene expression during development in vivo and in vitro. *Circ. Res.* 71(5):1021–30
19. Gasser JT, Chiesi MP, Carafoli E. 1986. Concerted phosphorylation of the 26-kilodalton phospholamban oligomer and of the low molecular weight phospholamban subunits. *Biochemistry* 25(23):7615–23
20. Gregoret LM, Rader SD, Fletterick RJ, Cohen FE. 1991. Hydrogen bonds involving sulfur atoms in proteins. *Proteins* 9(2):99–107
21. Harrer JM, Kranias EG. 1994. Characterization of the molecular form of cardiac phospholamban. *Mol. Cell. Biochem.* 140(2):185–93
22. Harrick NJ. 1967. *Internal Reflection Spectroscopy.* New York: Interscience
23. Holtzhauer M, Sydow H, Grunow G, Will H. 1986. Purification of phospholamban and characterization of its antibodies. *Biomed. Biochim. Acta* 45(6):719–25
24. Hubbard JA, MacLachlan LK, Meenan E, Salter CJ, Reid DG, et al. 1994. Conformation of the cytoplasmic domain of phospholamban by NMR and CD. *Mol. Membr. Biol.* 11(4):263–69
25. Huggins JP, England PJ. 1987. Evidence for a phosphorylation-induced conformational change in phospholamban from the effects of three proteases. *FEBS Lett.* 217(1):32–36
26. Huimin L, Thomas GJ Jr. 1991. Cysteine conformation and sulfhydryl interactions in proteins and viruses. 1. Correlation of the Raman S-H band with hydrogen bonding and intramolecular geometry in model compounds. *J. Am. Chem. Soc.* 113:56–62
27. Hwang KS, Nadal-Ginard B. 1991. Cloning phospholamban cDNA from rat aortic smooth muscle. *Adv. Exp. Med. Biol.* 304:387–95
28. Imagawa T, Watanabe T, Nakamura T. 1986. Subunit structure and multiple phosphorylation sites of phospholamban. *J. Biochem. (Tokyo)* 99(1):41–53
29. Inui M, Kadoma M, Tada M. 1985. Purification and characterization of phospholamban from canine cardiac sarcoplasmic reticulum. *J. Biol. Chem.* 260(6):3708–15
30. James P, Inui M, Tada M, Chiesi M, Carafoli E. 1989. Nature and site of phospholamban regulation of the Ca^{2+} pump of sarcoplasmic reticulum. *Nature* 342(6245):90–92
31. Jhun E, Jhun BH, Jones LR, Jung CY. 1991. Direct effects of ionizing radiation on integral membrane proteins. Noncovalent energy transfer requires specific interpeptide interactions. *J. Biol. Chem.* 266(15):9403–7
32. Johns DC, Feldman AM. 1992. Identification of a highly conserved region at the 5′ flank of the phospholamban gene. *Biochem. Biophys. Res. Commun.* 188(2):927–33
33. Jones LR, Simmerman HK, Wilson WW, Gurd FR, Wegener AD. 1985. Purification and characterization of phospholamban from canine cardiac sarcoplasmic reticulum. *J. Biol. Chem.* 260(12):7721–30
34. Jones LR, Wegener AD, Simmerman HK. 1988. Purification of phospholamban from canine cardiac sarcoplasmic reticulum vesicles by use of sulfhydryl group affinity chromatography. *Meth. Enzymol.* 157:360–69

35. Kalnin NN, Baikalov IA, Venyaminov SY. 1990. Quantitative IR spectrophotometry of peptide compounds in water (H_2O) solutions. III. Estimation of the protein secondary structure. *Biopolymers* 30(13–14):1273–80
36. Katz AM, Tada M, Kirchberger MA. 1975. Control of calcium transport in the myocardium by the cyclic AMP-protein kinase system. *Adv. Cyclic Nucleotide Res.* 5:453–72
37. Kauppinen JK, Moffatt DJ, Mantsch HH, Cameron DG. 1982. Fourier self-deconvolution; a method for resolving intrinsically overlapped bands. *Appl. Spectrosc.* 35:271–76
38. Kerr ID, Sankararamakrishnan R, Smart OS, Sansom MS. 1994. Parallel helix bundles and ion channels: molecular modeling via simulated annealing and restrained molecular dynamics. *Biophys. J.* 67(4):1501–15
39. Kim HW, Steenaart NA, Ferguson DG, Kranias EG. 1990. Functional reconstitution of the cardiac sarcoplasmic reticulum Ca^{2+}-ATPase with phospholamban in phospholipid vesicles. *J. Biol. Chem.* 265(3):1702–9
40. Kirchberger MA, Antonetz T. 1982. Phospholamban: dissociation of the 22,000 molecular weight protein of cardiac sarcoplasmic reticulum into 11,000 and 5,500 molecular weight forms. *Biochem. Biophys. Res. Commun.* 105(1):152–56
41. Kirchberger MA, Tada M, Katz AM. 1975. Phospholamban: a regulatory protein of the cardiac sarcoplasmic reticulum. *Recent Adv. Stud. Cardiac Struct. Metal* 5:103–15
42. Kovacs RJ, Nelson MT, Simmerman HK, Jones LR. 1988. Phospholamban forms Ca^{2+}-selective channels in lipid bilayers. *J. Biol. Chem.* 263(34):18364–68
43. Lamers JM, Stinis JT. 1982. Phosphorylation of low-molecular-weight proteins in preparations of rat heart sarcolemma and sarcoplasmic reticulum. *Adv. Myocardiol.* 3:289–97
44. Leberer E, Hartner KT, Brandl CJ, Fujii J, Tada M, et al. 1989. Slow/cardiac sarcoplasmic reticulum Ca^{2+}-ATPase and phospholamban mRNAs are expressed in chronically stimulated rabbit fast-twitch muscle. *Eur. J. Biochem.* 185(1):51–54
45. Le Peuch CJ, Le Peuch DA, Demaille JG. 1980. Phospholamban, activator of the cardiac sarcoplasmic reticulum calcium pump. Physicochemical properties and diagonal purification. *Biochemistry* 19(14):3368–73
46. Li T, Bamford DH, Bamford JK, Thomas GJ Jr. 1992. Cysteine conformation and sulfhydryl interaction in proteins and viruses. 2. Normal coordinate analysis of the cysteine side chain in model compounds. *J. Am. Chem. Soc.* 114:7463–69
47. Louis CF, Maffitt M, Jarvis B. Factors that modify the molecular size of phospholamban, the 23,000-dalton cardiac sarcoplasmic reticulum phosphoprotein. *J. Biol. Chem.* 257(24):15182–86
48. Ludlam CFC, Arkin IT, Liu X, Rothman MS, Rath P. et al. 1996. FTIR spectroscopy and site-directed isotope labeling as a probe of local secondary structure in the transmembrane domain of phospholamban. *Biophys. J.* 70:1728–36
49. Nicholls A, Honig B. 1992. *GRASP a Manual.* New York: Columbia Univ. Press
50. Otsu K, Fujii J, Periasamy M, Difilippantonio M, Uppender M, et al. 1993. Chromosome mapping of five human cardiac and skeletal muscle sarcoplasmic reticulum protein genes. *Genomics* 17(2):507–9
51. Park K, Perczel A, Fasman GD. 1992. Differentiation between transmembrane helices and peripheral helices by the deconvolution of circular dichroism spectra of membrane proteins. *Protein Sci.* 1(8):1032–49
52. Patai S. 1974. *The Chemistry of the Thiol Group.* London: Wiley
53. Perez-Gil J, Cruz A, Casals C. 1993. Solubility of hydrophobic surfactant proteins in organic solvent/water mixtures. Structural studies on SP-B and SP-C in aqueous organic solvents and lipids. *Biochim. Biophys. Acta* 1168(3):261–70
54. Raeymaekers L, Jones LR. 1986. Evidence for the presence of phospholamban in the endoplasmic reticulum of smooth muscle. *Biochim. Biophys. Acta* 882(2):258–65
55. Reddy LG, Jones LR, Cala SE, O'Brian JJ, Tatulian SA, Stokes DL. 1995. Functional reconstitution of recombinant phospholamban with rabbit skeletal Ca^{2+}-ATPase. *J. Biol. Chem.* 270(16):9390–7
56. Rothschild KJ, Clark NA. 1979. Polarized infrared spectroscopy of oriented purple membrane. *Biophys. J.* 25:473–88
57. Simmerman HK, Collins JH, Theibert JL, Wegener AD, Jones LR. Sequence analysis of phospholamban. Identification of phosphorylation sites and two major structural domains. *J. Biol. Chem.* 261(28):13333–41
58. Simmerman HK, Kobayashi YM, Autry JM, Jones LR. 1996. A leucine zipper stabilizes the pentameric membrane domain of phospholamban and forms a

coiled-coil pore structure. *J. Biol. Chem.* 271(10):5941–46
59. Simmerman HK, Lovelace DE, Jones LR. 1989. Secondary structure of detergent-solubilized phospholamban, phosphorylatable, oligomeric protein of cardiac sarcoplasmic reticulum. *Biochim. Biophys. Acta* 997(3):322–29
60. Suzuki T, Lui P, Wang JH. 1987. Rapid purification of phospholamban by monoclonal antibody immunoaffinity chromatography. *Biochem. Cell. Biol.* 65(4): 302–9
61. Tada M, Inui M, Yamada M, Kadoma M, Kuzuya T. et al. 1983. Effects of phospholamban phosphorylation catalyzed by adenosin 3′:5′-monophosphate- and calmodulin-dependent protein kinases on calcium transport ATPase of cardiac sarcoplasmic reticulum. *J. Mol. Cell. Cardiol.* 15(5):335–46
62. Tadesse L, Nazarbaghi R, Walters L. 1991. Isotopically enhanced infrared spectroscopy: a novel method for examining secondary structure at specific sites in conformationally heterogeneous peptides. *J. Am. Chem. Soc.* 113:7036–37
63. Tatulian SA, Jones LR, Reddy LG, Stokes DL, Tamm LK. Secondary structure and orientation of phospholamban reconstitute in supported bilayers from polarized attenuated total reflection FTIR spectroscopy. *Biochemistry* 34(13):4448–56
64. Terzi E, Poteur L, Trifilieff E. 1992. Evidence for a phosphorylation-induced conformational change in phospholamban cytoplasmic domain by CD analysis. *FEBS Lett.* 309(3):413-16
65. Thanabal V, Omecinsky DO, Reily MD, Cody WL. The ^{13}C chemical shifts of amino acids in aqueous solution containing organic solvents: application to the secondary structure characterization of peptides in aqueous trifluoroethanol solution. *J. Biomol. NMR* 4(1):47–59
66. Toyofuku T, Zak R. 1991. Characterization of cDNA and genomic sequences encoding a chicken phospholamban. *J. Biol. Chem.* 266(9):5375–83
67. Uyeda A, Kitano K, Fujii J, Kadoma M, Tada M, Tanaka S. 1986. Characterization of recombinant cDNA clones for canine cardiac phospholamban. *Nucleic Acids Symp. Ser.* (17):121–24
68. Uyeda A, Kitano K, Fujii J, Kadoma M, Tada M, Tanaka S. 1987. The cDNA sequence of the major phospholamban mRNA in canine cardiac ventricular muscle. *Nucleic Acids Res.* 15(16):6738
69. Venyaminov SY, Kalnin NN. 1990. Quantitative IR spectrophotometry of peptide compounds in water (H_2O) solutions. I. Spectral parameters of amino acid residue absorption bands. *Biopolymers* 30(13–14):1243–57
70. Venyaminov SY, Kalnin NN. 1990. Quantitative IR spectrophotometry of peptide compounds in water (H_2O) solutions. II. Amide absorption bands of polypeptides and fibrous proteins in alpha-, beta-, and random coil conformations. *Biopolymers* 30(13–14):1259–71
71. Verboomen H, Wuytack F, Eggermont JA, De Jaegere S, Missiaen L, et al. 1989. cDNA cloning and sequencing of phospholamban from pig stomach smooth muscle. *Biochem. J.* 262(1):353–56
72. Vorherr T, Wrzosek A, Chiesi M, Carafoli E. 1993. Total synthesis and functional properties of the membrane-intrinsic protein phospholamban. *Protein Sci.* 2(3):339–47
73. Watanabe Y, Kijima Y, Kadoma M, Tada M, Takagi T. 1991. Molecular weight determination of phospholamban oligomer in the presence of sodium dodecyl sulfate: application of low-angle laser light scattering photometry. *J. Biochem.* (*Tokyo*) 110(1):40–45
74. Wegener AD, Simmerman HK, Liepnieks J, Jones LR. 1986. Proteolytic cleavage of phospholamban purified from canine cardiac sarcoplasmic reticulum vesicles. Generation of a low resolution model of phospholamban structure. *J. Biol. Chem.* 261(11):5154–59
75. Wegener AD, Simmerman HK, Lindemann JP, Jones LR. 1989. Phospholamban phosphorylation in intact ventricles. Phosphorylation of serine 16 and threonine 17 in response to beta-adrenergic stimulation. *J. Biol. Chem.* 264(19):11468–74
76. Zhang YP, Lewis RN, Henry GD, Sykes BD, Hodges RS, McElhaney RN. 1995. Peptide models of helical hydrophobic transmembrane segments of membrane proteins. 1. Studies of the conformation, intrabilayer orientation, and amide hydrogen exchangeability of Ac-K2-(LA)12-K2-amide. *Biochemistry* 34(7):2348–61